AD-A163 984 LOW PASS FILTERS WITH LINEAR PHASE(U) MASSACHUSETTS INST OF TECH LEXINGTON LINCOLN LAB R M LERNER 12 DEC 85 TR-729 ESD-TR-85-240 F19628-85-C-0002 1/1

UNCLASSIFIED F/G 9/5 NL

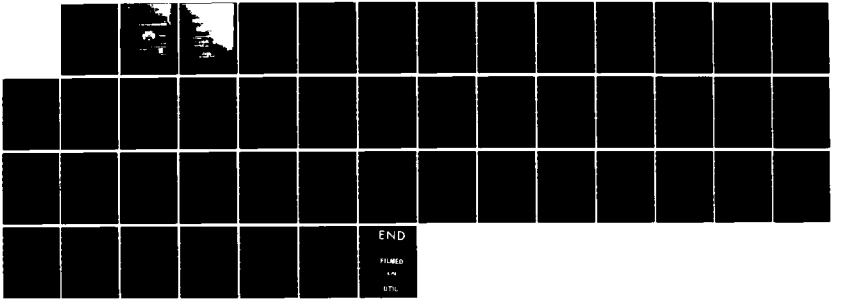

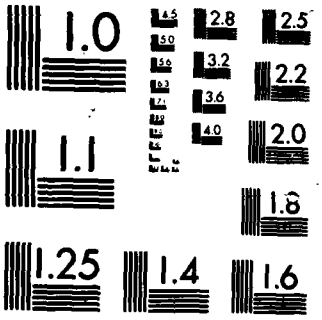

MICROCOPY RESOLUTION TEST CHART
NATIONAL BUREAU OF STANDARDS-1963-A

ESD-TR-85-340

Technical Report
729

Low Pass Filters with Linear Phase

DTIC
ELECTE
FEB 10 1986
S D

R.M. Lerner

12 December 1985

Lincoln Laboratory
MASSACHUSETTS INSTITUTE OF TECHNOLOGY
LEXINGTON, MASSACHUSETTS

Prepared for the Department of the Air Force
under Electronic Systems Division Contract F19628-85-C-0002.

Approved for public release: distribution unlimited.

AD-A163 984

DTIC FILE COPY

86 2 7 098

[redacted]

[redacted]

[redacted]

[redacted]

[redacted]

This technical report has been reviewed and is approved for publication.

FOR THE COMMANDER

Thomas J. Alpert

Thomas J. Alpert, Major, USAF
Chief, ESD Lincoln Laboratory Project Office

Non-Lincoln Recipients

PLEASE DO NOT RETURN

Permission is given to destroy this document when it is no longer needed.

MASSACHUSETTS INSTITUTE OF TECHNOLOGY
LINCOLN LABORATORY

LOW PASS FILTERS WITH LINEAR PHASE

R.M. LERNER

Division VI

TECHNICAL REPORT-729

12 DECEMBER 1985

Approved for public release; distribution unlimited.

LEXINGTON MASSACHUSETTS

ABSTRACT

This report is intended as a modern sequel to "Band Pass Filters with Linear Phase", published over 20 years ago. Here, the linear phase algorithms are adapted to low–pass integrated active circuit topologies for potential use as the input filter in sampled data control systems and other low–pass applications for which traditional coil–capacitor–transformer filter designs are no longer appropriate.

The linear phase algorithm is applicable to a variety of circuit topologies which are not mathematically equivalent. Application to the overall transfer function (the "simple" approach) results in transmission that is nearly equal–ripple in both amplitude and phase, the errors being equivalent to echos in a misterminated transmission line. The resulting filters compare favorably with modest order Tchebychef filters (lacking phase control). Application to branches of a feedback topology (mathematically equivalent to a lattice) leads to control of echoes and stop–band zeros at the cost of extra elements. In this case, the results compare favorably with ordinary Butterworth filters (lacking phase control) having the same total number of poles.

Practical means for inserting stop band zeros without redesign of the pass–band are considered. Circuits of both the R–C and switchcap types are discussed.

QUALITY INSPECTED 3

Accesion For
NTIS CRA&I ☒
DTIC TAB ☐
Unannounced ☐
Justification .....
By .....
Distribution /
Availability Codes
Dist | Avail and / or Special
A-1

CONTENTS

LIST OF ILLUSTRATIONS

LIST OF TABLES

Section 1

INTRODUCTION

Some years ago, the writer described algorithms for designing slab–sided flat–topped band–pass filters whose in–band phase response is an inherently linear function of frequency[1]. Elsewhere, he also disclosed adaptations of the algorithms to band–pass filters with quadratic phase[2] ("chirp" filters) and to non–integer power law impedances[3]. Colleagues independently adapted the linear phase technique to sampled data for use in Vocoders[4] and general digital filter design[5].

An application to the design of low–pass filters was promised [1] but was not published. A vigorous sampled data technology suggests examination of the low–pass linear phase filter as a means of prefiltering such data before, or concurrently with, sampling. Today, a high–Q single pole–pair is easily synthesized with op–amps, resistors, and capacitors, either as an analog feed–back network[6] [7], or as a switched capacitor network[8]. Such responses are easily joined with isolation amplifiers and summing nodes, all on a single integrated chip. This report emphasizes topologies appropriate to such active integrated circuit synthesis.

Figure 1 shows a typical amplitude template for specifying a single stage low pass linear phase filter. Here, M is the number of "main poles". A linear phase design also requires a minimum overhead of two "corrector poles".

The template differs from ordinary specification templates in (a) allowing a wider transition between the 1 dB point and the beginning of stop band roll–off, and (b) allowing an additional transition between the tolerance limits deep in band and the 1 dB point. The template includes the possibility a stop band zero for supressing carrier leakage. In–band, the phase is bounded by the same template, with 0.1 radian phase distortion replacing the 1 dB amplitude bound.

Linear Phase (L–Ph) designs compare favorably efficiency in use of numbers of elements with Butterworth filters for given tolerances of pass–band transmission and rapidity of reaching fixed stop band attenuation. Figure 2 shows a nearly maximally flat L–Ph filter transmission having 15 total poles in the s–plane (11 so–called main poles, a pair of "correctors," and a pair of "compensators"). Its transmission compares favorably with that of a Butterworth having 17 total poles. The linearity of the phase, within a few degrees of a pure delay over most of the pass–band is thus "for free".

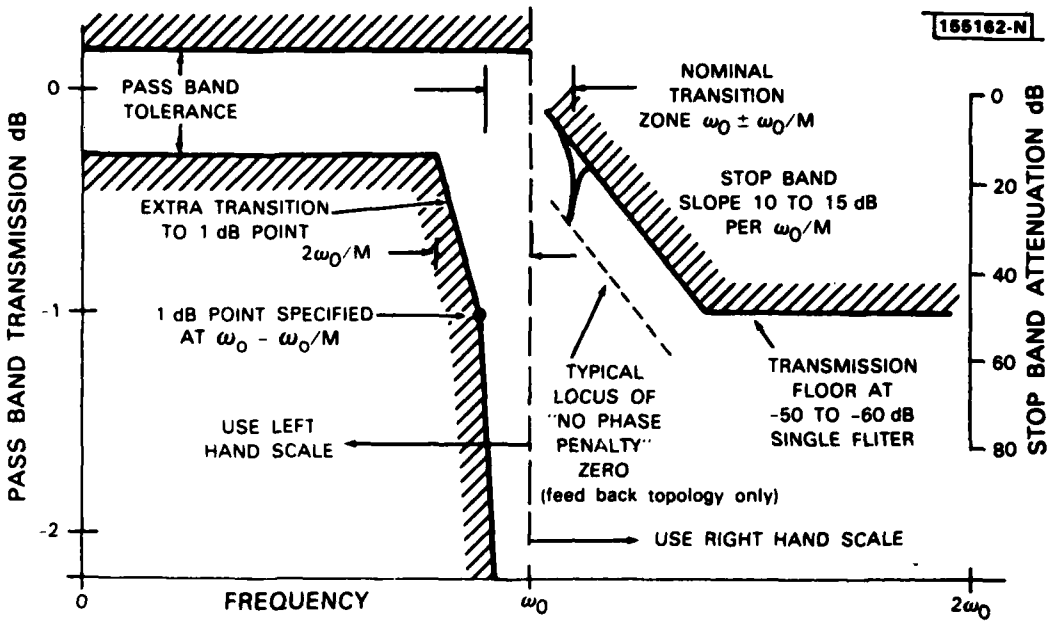

Figure 1. Template applicable to single stage linear phase filter. Stop band slope of template is 12.5M dB per ω_0.

Some of the results reported below appear to be new. These include the single and dual loop realizations of L–Ph lattice networks (Sections 2 and 8), details of manipulation of band–edge behavior (Section 5) and out–of–band zeros (Section 7). In addition, many results of computer simulation are presented, along with design equations which the reader can use to meet his own particular set of requirements.

There remains a widespread impression that phase linearity and pass–band squareness cannot be designed together. This impression is the legacy of an era in which filters were used almost exclusively for frequency division telephony, for which the notorious phase insensitivity of the ear led designers to concentrate on amplitude only. Even so, in a 1931 patent[9] Bode came very close to finding the L–Ph algorithms used here (he used pole–zero instead of pole–residue synthesis). The present writer believes that if serious commercial applications had then existed, Bode would have succeeded. It remains to be seen whether there are sufficient commercial applications to result in the widespread application of these techniques today.

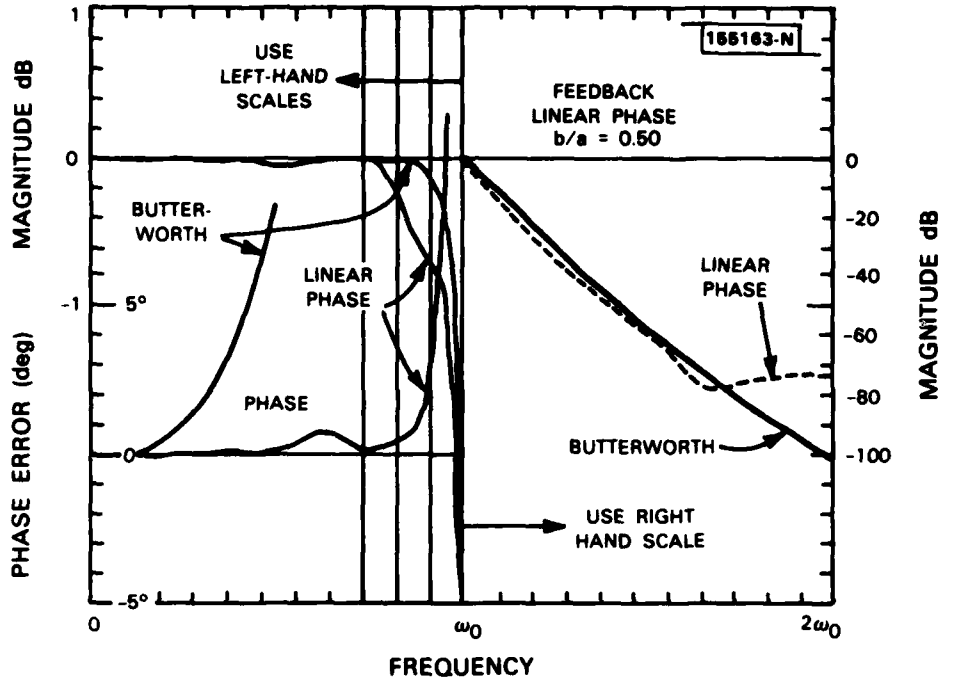

Figure 2. Comparison of Linear Phase with Butterworth designs. See Figure 13 for further details.

Section 2

NETWORK TOPOLOGY

Assume a mathematical description of a network as a rational transfer function H(w), often specified by its zeros and poles. The L–Ph design algorithms all specify the poles p_k and the residues r_k of the equivalent partial fraction expansion of H(w) [1][8]:

$$H(w) = c + r_1/(w-p_1) + r_2/(w-p_2) + \ldots + r_m/(w-p_m) \qquad (1)$$

The L–Ph algorithm was introduced in the s–plane. Gold and Rader [5], and recently Lish [8], have recognized that if the algorithm is applied in the z–plane, a sampled data L–Ph filter also results (although it is not exactly the same filter). The *w* in Eq (1) is intended to represent either the Laplace complex frequency *s*, $\sigma+j\omega$, or the sampled data transform variable *z*.

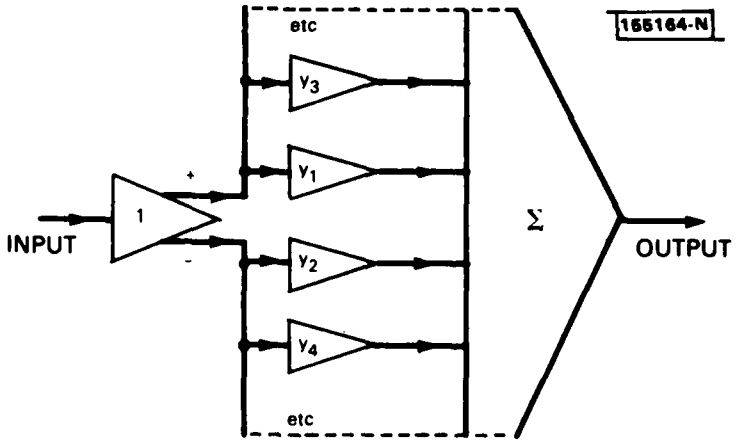

Figure 3. Topology for realizing H(w)

Figure 3 shows an active circuit version of the L–Ph filter topology based on the use of H(w) as a filter response. [1] This will be called the "simple" L–Ph filter topology. Each block represents an active circuit having the labelled transmission. Signal flow is in the direction of the arrows.

---

[1] The simple filters were called "infinite loss" filters in the original paper [1].

Physical realizability of H(w) requires that the individual terms occur in pairs having complex conjugate pole positions and residues. Each such pair is first summed to produce a physical 2nd order system y_i. (A pole on the real w-axis remains a 1st order system.) Those y_i of H(w) whose real part is positive near d.c. are driven from the "+" output of the input isolation stage. The sum will be called "Y_A". Those terms whose real part is negative near d.c. are driven from the "–" side; their sum will be called "Y_B". The individual transmissions are simply added to produce the output.

$$H(w) = Y_A(w) - Y_B(w) \qquad (2)$$

When the poles and residues of H(w) are chosen in accordance with the L–Ph algorithm below, the transmission of such a filter behaves like a finite–bandwidth section of transmission line with internal reflections from mistermination at the ends. These echos result in correlated nearly–equal ripple errors in both amplitude and phase within the pass band.

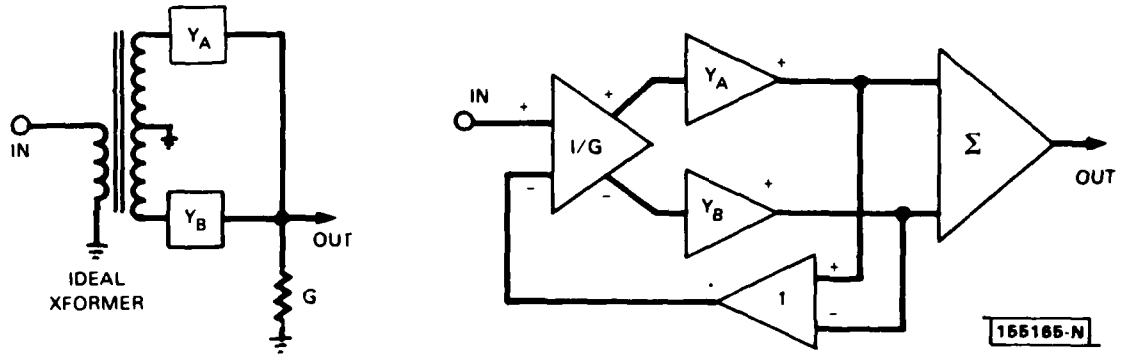

Figure 4. Realizations of the H(w) topology.
(a) "Low Loss" topology. (b) "Feedback" topology.

In addition to "simple" filters, the original paper explored the use of Y_A and Y_B as branch admittances feeding a load admittance G, as shown in Figure 4a. The corresponding active network will be called here the "feedback" or "loop" topology. When this new network is driven by a voltage source, the transmission is given by H(w)

$$H(w) = (Y_A - Y_B)/(Y_A + Y_B + G) \qquad (3)$$

Of course, this is *not* H(w). However, if Y_A and Y_B have been chosen according to the L–Ph algorithm, the resulting filter is L–Ph. Moreover, there is is a choice of G that terminates the equivalent delay cable and thus supresses the echos.

In general, G is the sum of a constant G_0 and a frequency dependent $G_p(w)$. It is evident from Eq (3) that H(w) will not change if only G_0 is assigned to the amplifier while $G_p/2$ is added to each of Y_A and Y_B. Such an assignment is convenient when G is also given in pole–residue form.

The original paper also considered a third generic network, having finite source impedance. Such a network is shown in circuit form on the left hand side of Figure 5. One reduction of this case to the feedback topology is shown in Figure 5. Two grand feedback loops are now required, and two extra frequency–dependent gain elements G. The Figure includes a reduction of G to the form of a fixed gain G_0 and feedback elements G_p.

The transmission of this new topology is given by H(w)

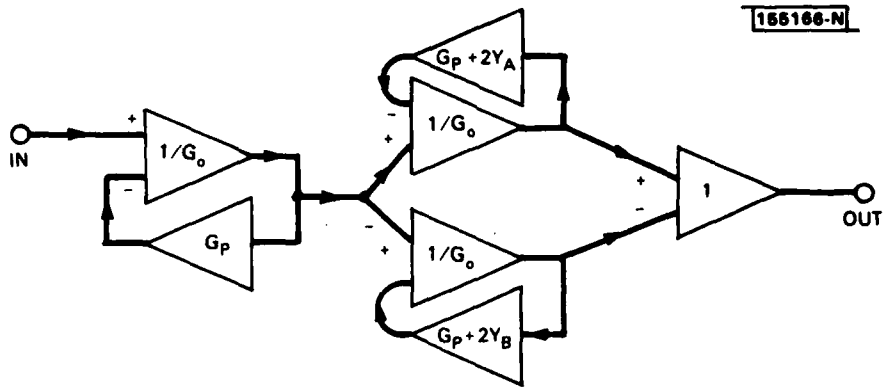

Figure 5. Matched source topology.

$$H(w) = 2(Y_A - Y_B)/(G+2Y_A)(G+2Y_B) \quad (4)$$

Both one loop and two loop topologies are treated further in Sections 6, 7, and 8 below.

Section 3

LINEAR PHASE ALGORITHM

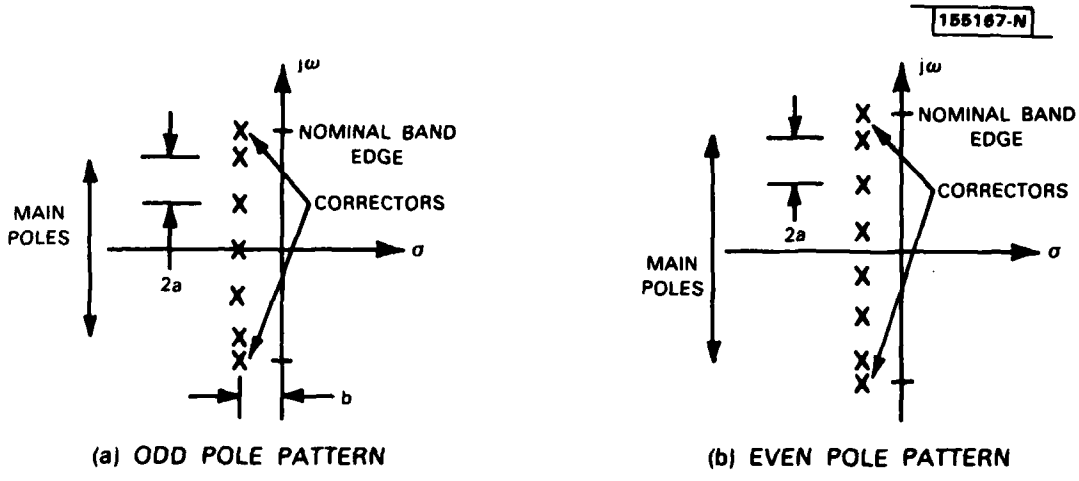

Figure 6. Allowable patterns for low pass poles.

The L–Ph design algorithm places all of the "main" poles at equal intervals $2a$ along a line parallel to the jω–axis in the s–plane, located at a distance b behind that axis. The residues at these poles all have the same magnitude; but residues at adjacent poles have alternating signs. Beyond upper and lower band edges, the line of main poles is simply stopped.

Nominal band edges at $\omega=\pm\omega_0$ are taken to lie half way between the last main and the first out–of–band pole of the periodic array. If there are M main poles (counting both half planes), then

$$\omega_0 = Ma \quad \text{or} \quad a = \omega_0/M \tag{5}$$

Let $E(j\omega)$ be the difference between the transmission of the main poles alone, and that of an infinite chain of such poles multiplied by an ideal slab–sided amplitude. In [1] it was shown that $E(j\omega)$ can be approximated by yet another pole located at each band edge, with a residue equal to one–half that of the first adjacent out–of–band pole dropped. These are the corrector poles. The nominal locations are on the same line as the main poles, at $s=\pm j\omega_0+b$.

For band-pass filters, the entire s-plane design is carried out in the upper half-plane. Physical reality requires another set of poles in the lower half plane. This merely adds another pass band at negative frequencies, whose skirts are too low to affect the transmission of the design filter (and vice versa). At low pass, the physical requirement of conjugate residues at conjugate pole positions can conflict with the L-Ph requirement for alternating signs at adjacent pole positions. Only two patterns of low-pass pole positions satisfy both sets of requirements: an even pole number pattern and an odd number pattern. Both are shown in Figure 6.

The usual pattern is that with an odd number of poles, which includes one pole on the real axis. All of the examples in this report are calculated on the assumption that the number of poles is odd. The even-number pattern is useful mainly as a means of inducing ripple reduction in a cascade with a simple filter having an odd-number pole pattern. The even pattern is not applicable to loop topologies.

In all these formulations, there is an arbitrary scale factor, which has been set equal to *b* below. A single contribution to H(s) is thus y_m

$$y_m = (-j)^m \, b/(s-jma+b) \tag{6}$$

where *m* is an even integer between ±M for odd pole filters. The corrector residue is r_c

$$r_c = 0.5 \, (-j)^{M+1} \, b \tag{7}$$

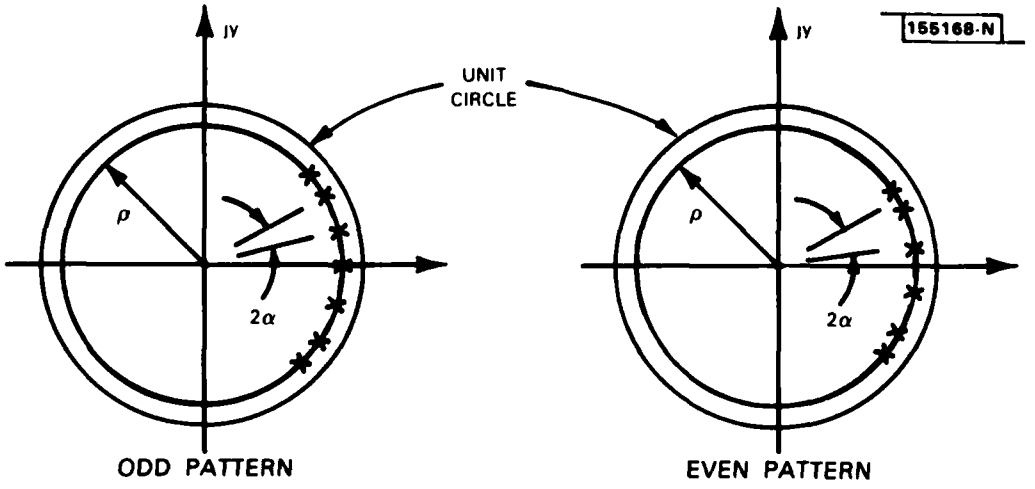

Figure 7. Position of low pass poles in z-plane.

Figure 7 shows the location of poles of a simple L-Ph filter specified directly in the z-plane. In this case, the main poles of H(z) are $y_m(z)$ They are located at equal intervals 2α along a circle whose center is at z=0.

$$y_m(z) = (-j)^m \rho/(z-e^{jm\omega}+\rho) \quad (8)$$

where $\rho<1$ is the radius of the pole circle. Lish [8] noted the explicit transformation between such a a z–plane design and an s–plane design:

$$z = e^{s\tau} \quad \text{or} \quad s = (1/\tau)\log(z) \quad (9)$$

where τ is the sampling interval in the time domain.

However, the simple s–plane and z–plane designs are not the same filter. The s–plane design that would correspond to Lish's simple z–plane filter has *periodic* pass bands at intervals of $1/\tau$ in radian frequency. This periodicity of pass bands will be dealt with later, in Section 10.

Section 4

SIMPLE FILTER

The L–Ph algorithm defines a pass band H(w) that is nearly periodic.

$$H(s) = \Sigma(-1)^k \, b/(s+b-2jka) \qquad \text{for odd pole filters}$$

$$H(s) = \Sigma(-1)^k \, jb/(s+b-j(2k+1)a) \qquad \text{for even pole filters} \tag{10}$$

If there are no limits on the k's, Eqs (10) can be summed to a closed form[10].

$$H(s) = \pi b/[2a \sinh(\pi(s+b)/2a)] \qquad [\text{odd}] \tag{a}$$

$$H(s) = \pi b/[2a \cosh(\pi(s+b)/2a)] \qquad [\text{even}] \tag{b}$$

(11)

From these equations it follows that the maxima H_{max} and minima H_{min} of transmission are

$$H_{max} = \pi b/2a \sinh(\pi b/2a)$$

$$H_{min} = \pi b/2a \cosh(\pi b/2a) \tag{12}$$

It also follows that the ratio of the squared magnitudes of maximum to minimum periodic transmission is $1+\epsilon^2$, where

$$\epsilon = 1/\sinh(\pi b/2a)$$

$$\sim 2\, e^{-\pi b/2a} \tag{13}$$

The last two equations state that low ripple is accompanied by low absolute transmission resulting from the small differences between overlapping y_i. Thus the design is subject to a tradeoff between low theoretical ripple and sensitivity to errors in the individual y_i. To aid the selection of b/a, Figure 8 gives the average magnitude $|H(j\,\omega)|$ and the amplitude of the fundamental component of the ripple as functions of b/a.

Figure 9 exhibits typical simple L–Ph filter responses with nominal correctors. That transmission does not quite fit the template in Figure 1. This can be cured by minor adjustments to the corrector, discussed in the next section. The Figure includes the result of one such adjustment; another is shown in Figure 11. Such corrector modifications have limited scope. For applications which require robust suppression of apparent echos, carrier leakage, or out of band interference, it is necessary to use cascades of filters and/or filters in the loop configurations.

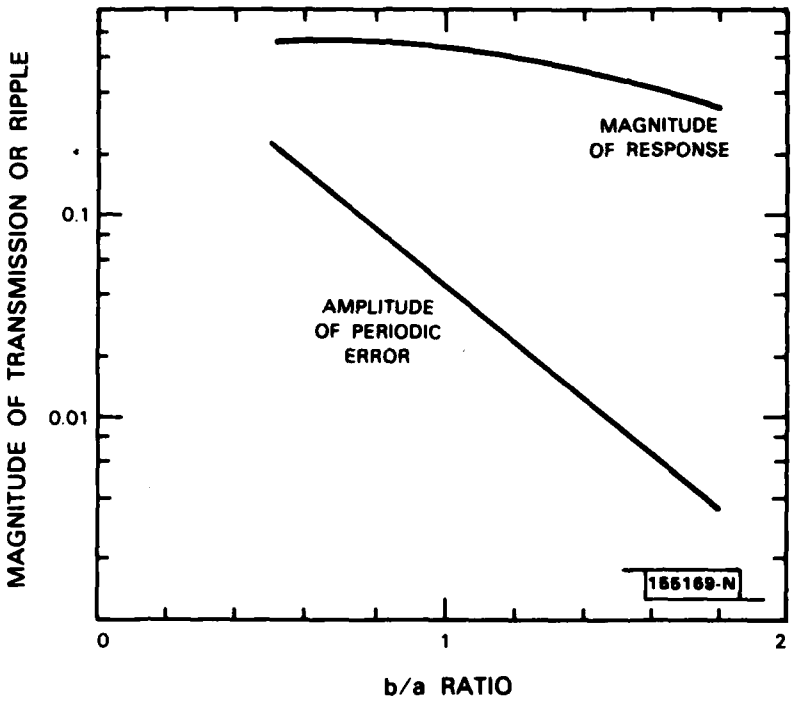

Figure 8. Design data for selection of b/a.

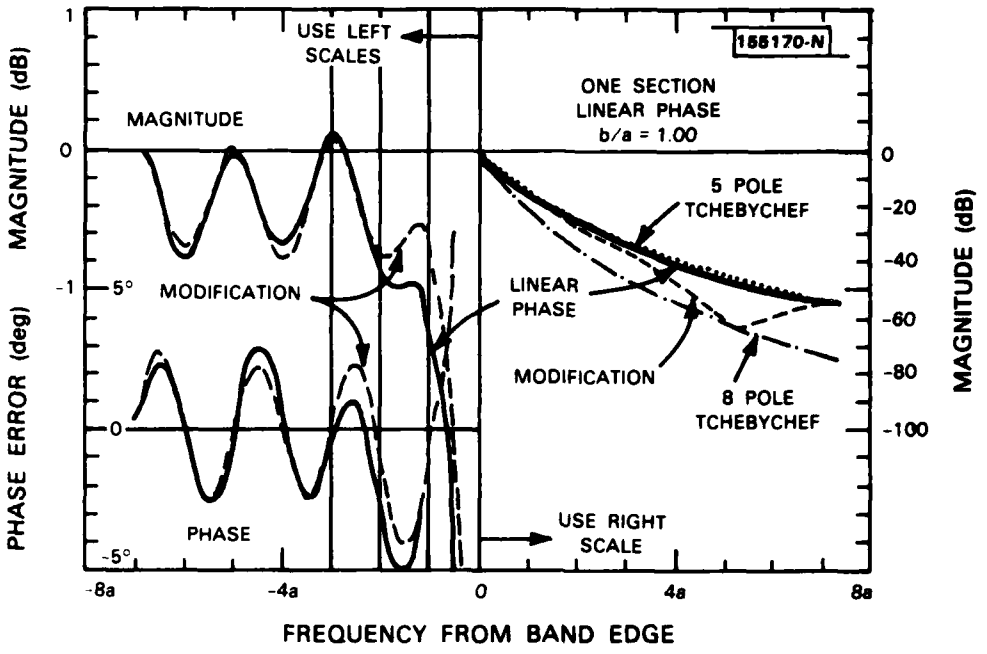

Figure 9. Response of filter near band edge.
Nominal corrector position and residue.
Corrector modified to 95% residue, 95% b, and position 0.1a out-of-band also shown.

4.1 COMPARISON WITH ORDINARY TCHEBYCHEF

It is natural to compare the transmission of the nearly equi-ripple simple L-Ph filter to that of the standard equi-ripple Tchebychef for phase distortion in-band and attenuation slope at the onset of the stop band. The comparison is made difficult by differences in the scaling rules for the design of the two filter types.

Except when M is small enough to produce special cases (M<5), the phase distortion of the L-Ph design occurs within $1.5\,\omega_0/M$ of the band edge at ω_0, while the stop band behavior is generally a function of η

$$\eta = M(\omega-\omega_0)/\omega_0 \qquad (14)$$

In particular, the nominal template stop band attenuation, Figure 1, is given, near the band edge,[2] by $W(\eta)$

---

[2] Observe that this is *not* the result of analysis of a given filter, but rather a specification slope.

$$|W(\eta)|^2 \leq e^{-2.9\eta} \tag{15}$$

On the other hand, the transmission $T(j\omega)$ of an N–pole Tchebychef is given by

$$|T(j\omega)|^2 = [1 + \epsilon^2 \cosh^2 N\cosh^{-1}(1+\eta/M)]^{-1} \tag{16}$$

Evidently, this transmission depends on ϵ, M, and N, as well as η, where that of the L–Ph can be specified in terms of η only.

To cast the preceding result into a form in which it can be compared directly with Eq (15), one can make use of the approximation [3]

$$\cosh^{-1}(1+u) = (2u)^{1/2} + \text{.....higher order terms in } u^{1/2} \tag{17}$$

$$\cosh^{-1}(1+\eta/M) = (2\eta/M)^{1/2} + \text{.....} \tag{18}$$

to obtain

$$|T(j\omega)|^2 \rightarrow (4/\epsilon^2) \exp[-2N(2\eta/M)^{1/2}] \tag{19}$$

Obviously, this result and Eq (15) are not comparable. For any ϵ it is always possible to find an N such that the Tchebychef attenuation lies either above or below the M–pole L–Ph for the first 50 dB of attenuation, and vice versa.

Figure 9 also shows the stop band transmission of two standard Tchebychefs having the same in–band ripple and a slightly narrower nominal bandwidth. Curves are plotted on the assumption that M≈N, so that number of L–Ph main poles equals the number of Tchebychef poles. The L–Ph stop band attenuation shown is bounded by that of 5– and 8–pole Tchebychefs out to a point at which the L–Ph filter "bottoms out" (either by design or on account of random construction errors). other situations. If the b/a in the figure had been 1.25, the bounding Tchebychefs occur at 8– and 11–pole; if b/a had been 1.50, the bounding Tchebychefs occur at 11– and 15–pole.

The phase distortion of a Tchebychef is simpler than its attenuation. It oscillates around an overall distortion curve Δ

$$\Delta = M [\arcsin(\omega/\omega_0) - \omega/\omega_0] \tag{20}$$

The onset of unacceptable phase distortion thus occurs deeper into the pass–band as N is increased. If for comparison with L–Ph, the edge of unacceptable phase distortion is taken to be at 0.1 radian distortion, then this edge occurs at ω/ω_0 of roughly 0.5 for a 5–pole and roughly 0.4 for a 8–pole Tchebychef. In contrast, in the L–Ph filter, as the number of main poles M is increased the span of acceptable phase distortion moves closer to the band edge; for a 0.1 radian limit, the phase distortion is satisfactory over (M–1)/M of ω_0.

---

[3] Higher order terms in the expansion can be obtained using the identity
$\cosh^{-1}(1+y) = \sinh^{-1}((2y+y^2)^{1/2})$
together with the power series expansion
$\sinh^{-1}(x) = x - x^3/6 + 3x^5/40 - \text{.....}$

Section 5

MODIFICATIONS OF SIMPLE FILTERS

This section considers several methods of tailoring the response of simple filters by adjustment of the corrector poles and by use of higher order correction.

The correctors y_c are an approximation to the ideal difference $E(j\omega)$. Figure 10 shows the real and imaginary parts of typical $E(j\omega)$, and of corresponding nominal correctors Y_c.[4] The left hand side of the Figure illustrates b/a less than one. The right hand side is typical of b/a>1. (The right hand amplitude scales have been expanded to show the approximation error on the same *relative* scale as for b/a=0.5). In both cases, the missing halves of the curves are obtained by reflection with respect to the band edge, with the imaginary parts changing sign. In the 1930s Bode[11] gave relationships that hold along $s=j\omega$ between the real and imaginary parts of physically realizable H(s). Key concepts included minimum phase for a given gain curve, maximum loss for a given phase curve, minimum reactance for a given real part, and various Hilbert Transform[5] relationships between real and imaginary parts when one or the other is specified for all frequency.

Although Re(E) and Im(E) have the correct general relationship for physical realizability, $E(j\omega)$ is not "minimum reactance". It follows that there is no *physical* "super-corrector" arbitrarily close to $E(j\omega)$ for all frequencies. The curve labelled "HT" shows the minimum reactance imaginary part for Re(E) when b/a =0.5, obtained from Re(E) by numerical Hilbert transform.

However, excellent correction can be obtained outside a transition zone straddling the band edge. In this report, the width of that zone is arbitrarily fixed to be $\pm a$ around ω_0.

Adjustments to the corrector pole(s) of a simple filter can effect modest tradeoffs between extending L-Ph into the transition zone (at the expense of increased attenuation in-band) versus extending the flat-topped amplitude response towards the band edge (at the cost of increased phase distortion). Most of the illustrative examples involve such adjustments to single pole correctors.

---

[4] A filter with an odd number of poles is assumed. If the number of poles is actually even, statements about "real" and "imaginary" parts must be interchanged. Such an interchange has no effect on the overall results.

[5] If F(x) is a suitably bounded generalized function, its Hilbert Transform G(x) is given by

$$G(x) = (1/\pi) \int F(u)du /(x-u)$$

where the integral is understood in the Cauchy (or generalized function) sense to run between $u=-\infty$ and ∞.

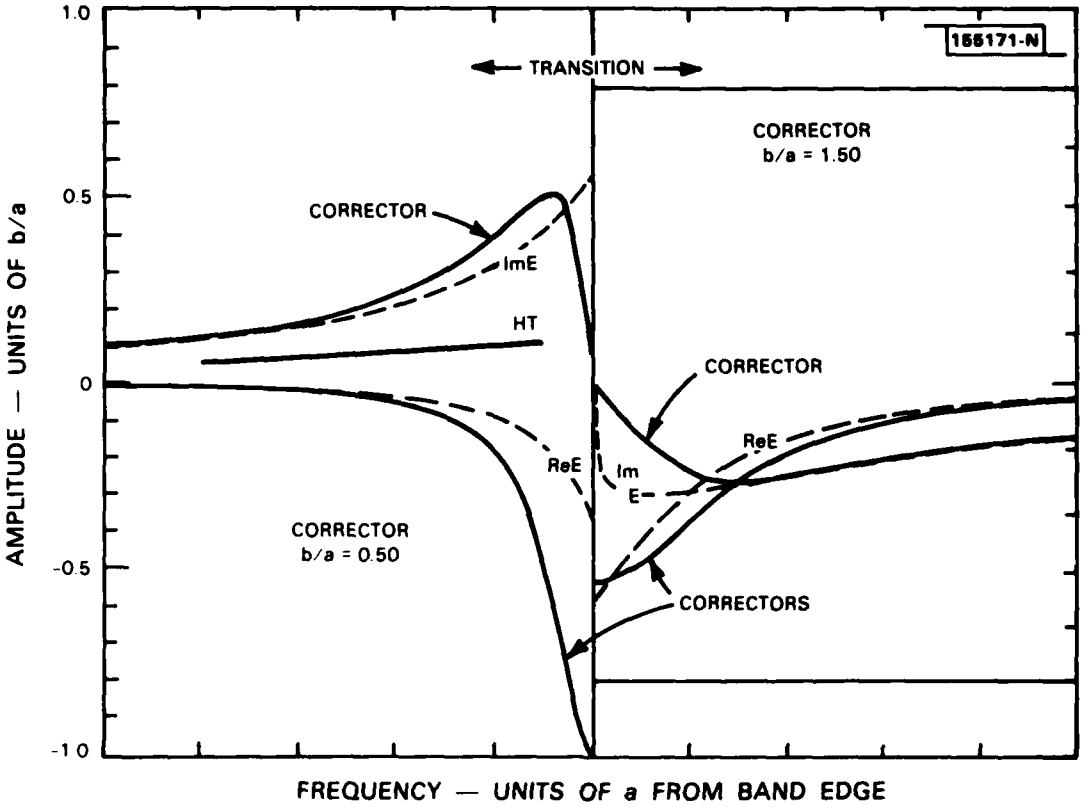

Figure 10. E(ω) and corrector functions.

5.1 ADJUSTMENT OF SIMPLE CORRECTOR POLE

The following observations can be used to guide adjustments to the residue or position of a single corrector pole to make minor local improvements to the match to E(j ω).

1. Reducing the corrector residue from nominal (½), improves the match of both real and imaginary parts near $\omega_0 \pm a$, at the expense of a broad "bottom" to the in-band ripple and stop band attenuation.

2. The primary effect of changing corrector *b* is to change the real part of y_c. Thus improving the knee of the pass-band at the zone edge generally involves lowering the *b* of the corrector pole.

3. Moving the frequency of the corrector (parallel to the j ω-axis or z-circle) improves the match of y_c and E(ω) close to one side of the transition zone, at the expense of the match on the other side of the zone.

As a rule, the illustrative examples of this report involve such adjustments to the corrector. For example, Figure 9 includes modifications to the corrector pole to make the in-band response conform to the template of Figure 1.

5.2 USE OF MULTIPLE POLE CORRECTORS

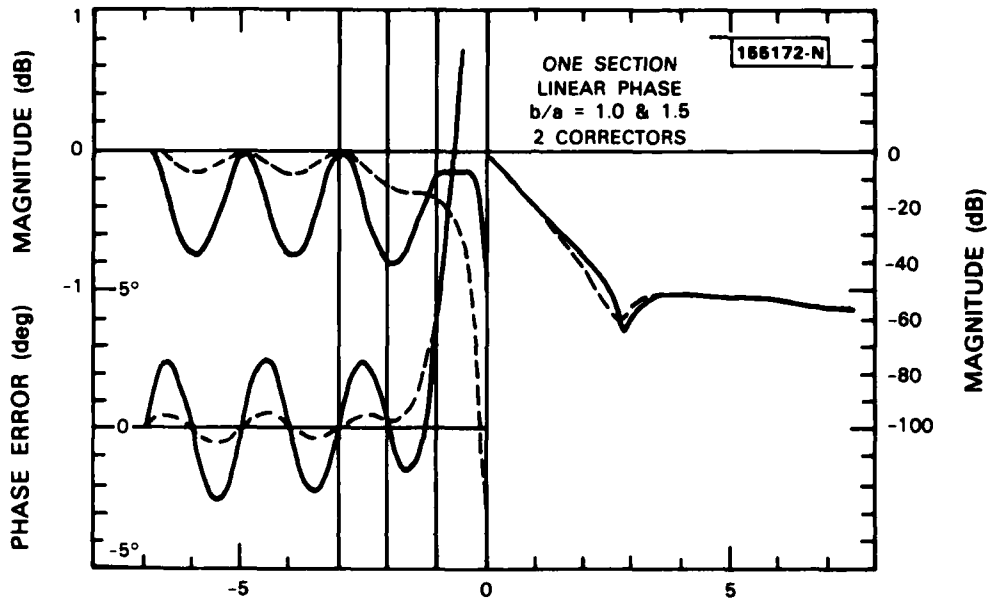

Figure 11. Use of two term corrector.

In the range $0.5<b/a<1.5$ two poles can be used in combination to produce a better match (outside the zone) to $E(j\omega)$ than is available from a single pole. Let the amplitudes of these two correctors be γ_1 and γ_2, and the damping b_1 and b_2:

$$y_{C1} = b\gamma_1 /(s^*+b_1)$$

$$y_{C2} = b\gamma_2 /(s^*+b_2) \qquad (21)$$

with the signs of the y's chosen to give the same sense as the nominal corrector. The most important on the γ's and b's is asymptotic equality of Im(E) and $Im(y_C)$. A less important constraint is the asymptotic equality of the real parts. Together, these constraints suffice to determine the γ's in terms of the b's:

$$\gamma_1 = (b-b_2)/(b_1-b_2)$$

$$\gamma_2 = (b-b_1)/(b_2-b_1) \qquad (22)$$

One strategy for choosing the b's is to chose one corrector pole to have the lowest b_1 that is consistent with practical hardware and boundedness of y_C in the transition

zone. The other pole is taken with a fairly large b_2 (say b/a=2.5). The gammas are calculated according to Eqs (22). Using this point of departure, a satisfactory set of b's and γ's is found by computer cut-and-try.

TABLE 1

Parameters for Two Pole Corrector

	b_1/a	γ_1	b_2/a	γ_2
Filter b/a=0.5	2.5	0.09	0.20	0.41
Eq(22)		0.065		0.435
Filter b/a=1.0	2.5	0.17	0.40	0.33
Eq(22)		0.143		0.357
Filter b/a=1.5	2.5	0.25	0.60	0.25
Eq(22)		0.237		0.263

Figure 11 shows the use of two pole correctors for y_c in simple L-Ph filters for b/a=1 and b/a=1.5. The actual cut-and-try parameters used are given in Table 1. The Table also lists corresponding γ's computed from Eqs (22). Note that the transmission of the filter for b/a =1 has lower distortion in-band and sharper attenuation skirts than attenuation out-of-band than either of the single pole adjustments shown in Figure 9.

How far can the multiple corrector pole approach be extended? For any given topology there is a minimum width of the transition, such that a corrector y_c which matches $E(j\omega)$ outside this zone will not produce unacceptable peaks in transmission within it. Theoretical specification of this minimum cannot be undertaken here. In fact, for low b/a, even the nominal corrector can cause unacceptable peaks or "ears" inside the transition zone, especially in the single loop feedback topology dicussed in Section 6.

Low b/a is not used in single simple filters. However, it is used in cascades and in loop topologies. Low b/a also lays bare character of the nominal transition zone edges. For b/a<<1, the $|Im(E)|$ tends to a limit of .349b/a at $\pm a$ from the band edge, while the $|Im(y_c)$ tends towards 0.5b/a. Both real parts tend to vanish. The result is a net residual imaginary part $\pm 0.151b/a$ at the zone edges. This can be compared with a periodic pass band minimum $|H(\omega)|$ of $\pi b/2a$ as $b/a \to 0$; and a periodic maximum Re(H) of unity.

Thus, the residual produces transmission at roughly -20 dB with respect to the pass band minima at the outer edge of the transition zone, and 0.15b/a radian phase distortion at the inner edge. The effect of these residuals can be reduced in general only by blunting the sharpness of the transition at the band edge by the use of high-b corrector elements, or by introducing unacceptable peaks within the zone.

Section 6

FEEDBACK TOPOLOGY

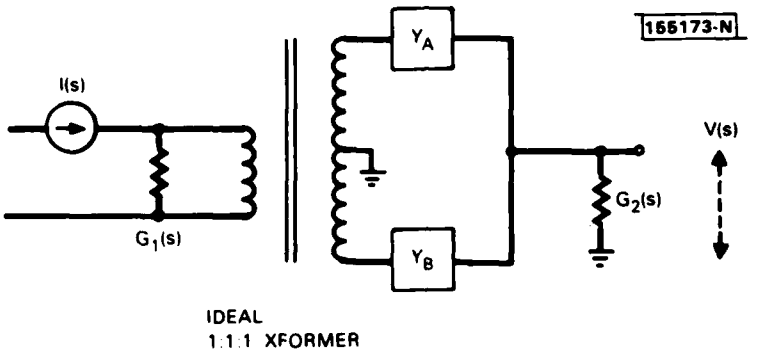

Figure 12. Lattice network.

Any passive bilateral network that can be inserted between a source having (complex) admittance G_1 and a load having impedance G_2 can be realized in the form of a half lattice, shown in Figure 12. [6] In the original paper it was shown that excellent L–Ph filters can be obtained in this topology by applying the L–Ph algorithm to Y_A and Y_B rather than to T(s). This use of the algorithm can be extended to low pass filters with an *odd* total number of poles.

Two special cases are of interest: the case of "matched" source and loads, $G_1=G_2=G$, and the low impedance source, $G_1=\infty$, $G_2=G$. For matched loads, the transmission has already been given as Eq (4). In the low impedance case ($G_1=\infty$) the current source is replaced by a voltage source. The transmission is given in Eq (3).

$$T(s) = (Y_A-Y_B)/[G+Y_A+Y_B] \qquad (3)$$

---

[6] In networks textbooks, main attention is usually given to is a full symmetric lattice with balanced inputs and outputs; the original paper made use of full lattice analysis. To compare equations, the half-lattice G's in this report are twice the full lattice G's of the original paper. Branch Y's are unchanged in meaning.

Let y_A and y_B be the infinite pole–residue arrays that are eventually truncated into the main poles of Y_A and Y_B. The echos in pass band transmission are eliminated by chosing G according to the image parameter rule

$$G^2 = 4y_A y_B \tag{23}$$

In particular, if the total number of main poles (after truncation) is odd, the individual y_A and y_B (as well as y_A–y_B) are periodic. They can be expressed in closed form as tangents. For example, if y_A happens to include the pole on the negative real axis:

$$y_A = \pm(\pi b/4a)\ \tanh((s+b)/4a)$$

$$y_B = \pm(\pi b/4a)\ \coth((s+b)/4a) \tag{24}$$

The periodic product $y_A y_B$ is independent of frequency. The image admittance G reduces to G_0

$$G_0 = \pi b/2a \tag{25}$$

Direct substitution of y_A, y_B, and G_0 from the preceding equations into Eqs (3) or (4) produces (after some complex variable trigonometry) a simple delay with attenuation independent of frequency.

$$T(s) = \text{constant x } e^{-\pi b/2a}\ e^{-\pi s/2a} \tag{26}$$

6.1 SHUNT COMPENSATION

In this subsection it is assumed that the branch Y_A contains the main pole(s) closest to the band edge and that Y_B contains the corrector pole(s), y_C.[7] Let y^*_A and y^*_B represent the periodic poles that are dropped when the network is truncated:

$$Y_A = y_A - y^*_A \qquad \text{(main poles)} \tag{a}$$

$$Y_B = y_B - y^*_B + y_C \qquad \text{(main poles plus corrector)} \tag{b}$$

$$G = G_0 + G_p \tag{c}$$

(27)

The original paper points out that the choices

---

[7] If Y_B contains the pole closest to band edge, Y_A includes the corrector, and G_p is made up of the dropped terms y^*_B.

$$y_C = y^*_B - y^*_A \quad \text{(in band only)} \qquad \text{(a)}$$

$$= (y_A - y_B) - (y^*_A - y^*_B) \quad \text{(out of band)}$$

$$G_p = 2y^*_A \qquad \text{(b)}$$

(28)

produce ideal pass–band transmission and stop–band attenuation. The reader can confirm this by using Eq (cpi) to reduce Eq (27), then substituting the result into either of Eqs (22). The actual corrector is an approximation to Eqs (28a) and (28b). *Proper selection of the corrector* is all that is needed to convert the filter from *infinite bandwidth* to *design bandwidth.*

Eq (27c) introduces a second kind of corrector, called in the original paper "shunt compensation," G_p. Ideally, this new G_p is the sum of all the terms y^* that were dropped from y_A (but not y_B) when it was truncated from periodic to finite form. [7] The ideal G_p contains the poles located at M+3a, M+7a, ... and at –M–3a, –M–7a,.... This G_p can be expressed in closed form using the ψ–function (the logarithmic derivative of the Γ–function):

$$G_p = (b/2aj)\,[\psi((M+3)/4 - (s+b)/4aj) - \psi((M+3)/4 + (s+b)/4aj)] \qquad (29)$$

In practice, shunt compensation consists of a few network elements which approximate the ideal G_p in–band. Near d.c., G_p can be approximated by a nearly constant real part, and an imaginary part which varies linearly with frequency:

$$G_p = g_0\, b^2/a^2 + g_1 s\, b/a + ...$$

$$g_0 = 1/(M+1)^2 + ...$$

$$g_1 = 1/(M+1) - (2/3 + b^2/3a^2)/(M+1)^3 + ... \qquad (30)$$

Near the band edge, the simple power series development of G_p is not wholly adequate. In addition, the synthesis of the term $g_1 s$ is not convenient for the active feedback topology. It is better to use an out–of–band pole pair, even when the resulting zero in transmission is not the primary objective.

The parameters of a one pole pair G_p can be computed using Eq (29).[8] The frequency and residue are chosen so that $\mathrm{Im}(G_p)$ has the correct value at the in–band edge of the transition zone (at $s^* = ja$), and the correct slope at d.c. The damping of

---

[8] The properties of the ψ–function are discussed in standard treatments of higher transcendental functions. For $\mathrm{Re}(w) > 0$, $\psi(w)$ is $\ln(w) - 1/2w - d\Upsilon(w)/dw$ where $\Upsilon(w)$ is a continued fraction. (*Handbook of Mathematical Functions*, Abramowitz and Stegun, Editors, Dover, New York, 1970, §6.1.48). In reducing formulas, the author has used the recursion (*op cit* §6.3.5):

$\psi(z) = -1/z + \psi(z+1)$

an asymptotic expansion for $d\psi/dz$ (from *op cit* §6.4.12):

$\psi'(z) = 1/(z-½) - 1/24(z-1/2)^3 + ...$

and his own formula for numerical computations:

$\psi(x) = \ln(x-.493) + 1/10x^3 \pm 0.0003$ for $x > 1.1$

the pole pair is next selected to produce the proper real part for G_p at the zone edge. Finally, g_o is adjusted so that the real part is correct at d.c.

Let p and q be the normalized magnitudes of the real and imaginary parts of $E(j\omega)$ at the zone edge:

$$E(j\omega_o) = p\, b^2/a^2 - jq\, b/a \tag{31}$$

Approximate formulas for p and q are[8]

$$p = .198 + 1/4M - .026\, b^2/a^2$$

$$q = -0.0579 + \ln(M) - .040\, b^2/a \tag{32}$$

The result of the matching process just outlined is a pole pair given by parameters (A, B, C):

Locations at $s = Bb \pm j\,(M+A)a$ Residues = Cb

Table 2 gives values for A, B, and C calculated according to the above matching process for the case b/a=½. The numbers are not significantly different for any other b/a→0.

TABLE 2

Parameters of Nominal Compensation....b/a =½

M	q	A	A/q	C	B	ΔG_o
5	0.74	6.52	8.84	10.74	1.29	0.24
7	0.91	6.99	7.72	12.04	1.23	0.11
9	1.03	7.64	7.42	13.72	1.22	0.07
11	1.13	8.33	7.36	15.47	1.23	0.04
13	1.21	9.01	7.42	17.23	1.25	0.03
15	1.29	9.69	7.53	18.99	1.28	0.02
17	1.35	10.35	7.67	20.73	1.31	0.02
19	1.40	10.99	7.83	22.45	1.34	0.01
21	1.45	11.63	8.00	24.17	1.37	0.01

Figure 13 shows the transmission of a single loop feedback network with 11 main poles (5 each in upper and lower half planes) using compensation from Table 2 and nominal correctors. Figure 2 is similar. Here, corresponding curves are plotted for b/a equal to 0.25 and 0.50. Note that they are essentially identical. However, at b/a =0.25 there is a serious peak or "ear" in transmission, which gets worse as b/a is reduced. This peak is eliminated in the "matched" or "double loop" topology.

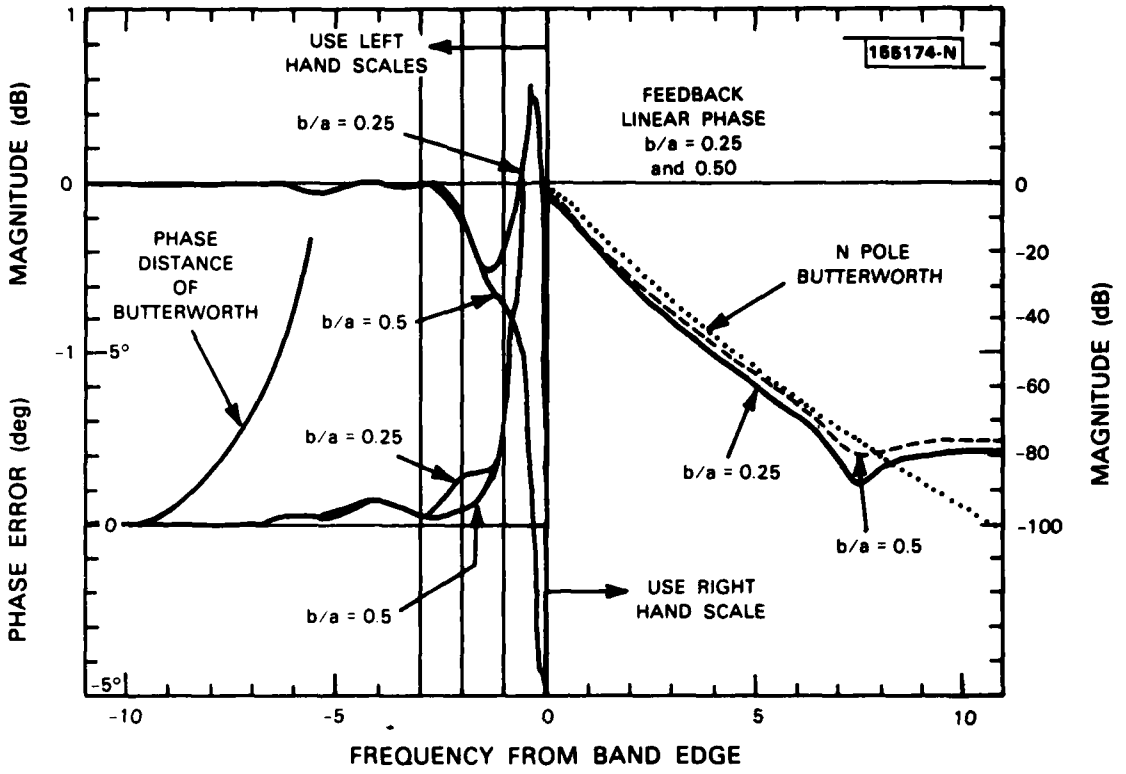

Figure 13. Feedback network with nominal compensation.

6.2 COMPARISON WITH BUTTERWORTH

Nominally, the transmission of a properly terminated loop topology L–Ph filter is flat within the pass band. This is especially true in practice with the two loop designs discussed in a later section, where both ends of the equivalent transmission line are, in effect, terminated. Such flat response invites comparison with the ordinary (maximally flat) Butterworth filter. Unlike the Tchebychef comparison earlier, the comparison is possible and uniformly favorable to the L–Ph for the same total number of poles utilized.

The specified stop–band attenuation slope of a L–Ph filter has already been set forth in Eq (15)

$$|W(\omega)|^2 \leq \exp(-2.9\eta) \tag{15}$$

The transmission of a Butterworth having N elements is B(ω)

$$
\begin{aligned}
|B(\omega)|^2 &= [1 + (\omega/\omega_0)^{2}N]^{-1} \\
&= [1 + \exp 2N\ln(\omega/\omega_0)]^{-1} \\
&= [1 + \exp 2N\ln(1+\eta/M)]^{-1} \\
&\rightarrow [1 + \exp 2N\eta/M]^{-1} \\
&\rightarrow \exp(-2N\eta/M) \qquad (33)
\end{aligned}
$$

Evidently, in both cases the attenuation slope follow the same scaling law. Observe that for a given slope, then number of L–Ph main poles is substantially less than the total poles of the Butterworth, so that the comparison can remain favorable to L–Ph even including correctors and compensators.

Figure 13 also compares the transmission and phase distortion of the L–Ph filter with the Butterworth filter whose transmission it most nearly resembles. This Butterworth has the same group delay at d.c. and virtually the same stop band transmission out to where the L–Ph filter "bottoms". It has $\pi M/2$ poles, rounded to the nearest integer. Allowing for the overhead of corrector and compensator, there are still just as few second order systems in the L–Ph filter!

The figure also shows the phase distortion of the Butterworth, which is similar to the average distortion of the Tchebychef. Note that it exceeds the 0.1 radian criterion near midband. Here, the comparison favors the L–Ph over the Butterworth on all practical counts. The price is inexact theoretical flatness, and the 1 dB shoulder within $2\omega_0$ of the band edge.

Section 7

ZEROS

In providing shunt compensation, zeros were inserted into the L–Ph stop band. The position and depth of such zeros do not depend on adjustments to main poles and correctors. The manipulation of such zeros is thus an important feature of feedback topology design.

7.1 NATURAL STOP BAND ZEROS

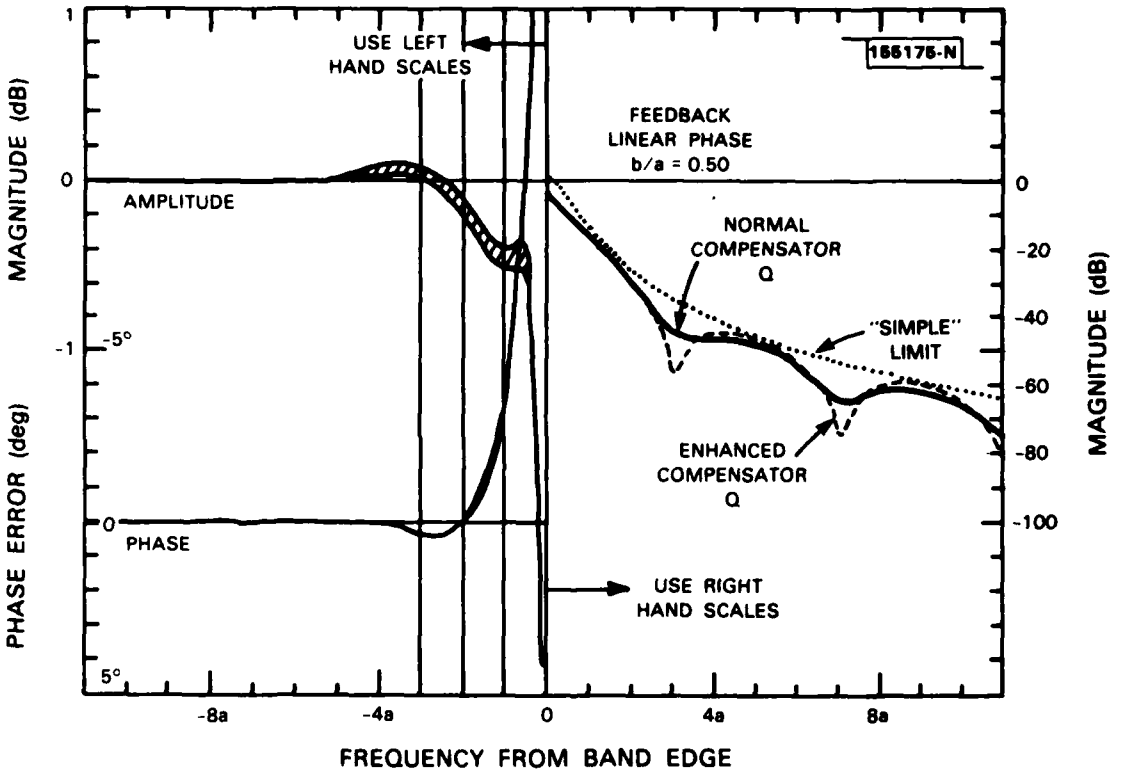

Figure 14. Effect of use of compensation with multiple poles. Corrector b/a 90% of nominal to sharpen 1 dB transition in-band

Figure 14 shows filter transmission with the "ideal" compensation G_p specified by Eq (28). Since Y_A and Y_B contain no poles in the stop band, the poles of G_p (in accordance with Eq (3)) insert zeros into the stop band transmission at regular intervals beyond the band edge. Compensation that was concentrated at a single zero in the stop band is now spread over several zeros. Up to the first zero the attenuation exceeds that for single element compensation. Beyond this point the loss proceeds in stair-step fashion and is not immediately as profound as for the single element.

Inasmuch as G_0 is also a part of G in the stop band, it follows from Eq (3) that the attenuation cannot be less than that of a simple filter $(Y_A-Y_B)/G_0$, whatever be the form of G_p, so long as Y_A, Y_B, and G_p are positive real (i.e. individually stable) elements. This minimum attenuation curve is also shown in the Figure. Using lower loss elements for the poles of G_p will result in deeper stop band zeros; but the maxima between zeros then tend to touch the minimum loss curve. There is also an adjustment to G_0 to avoid a reduction in Re(G) in the pass band.)

7.2 INSERTION OF ARBITRARY STOP BAND ZEROS

There are two separate stratagems available for the insertion of zeros into a L-Ph filter stop band. The first makes use of adjustments to the corrector; it is available in all cases. The second makes use of the compensation; it is available only in the feedback topologies.

It is always possible to pick the damping and residue of the corrector in such a way as to obtain equality of $E(j\omega)$ and Y_C at one frequency in the stop band (and at a corresponding frequency in the pass band). It is also possible to achieve the same result asymmetrically by adjusting corrector position instead of corrector damping. Such zeros are available in all L-Ph topologies because they affect only the Y_A-Y_B portions of the transmission equations.

However, the technique is sensitive to minor changes in component values. It is not useful for maintaining a zero against fixed carrier frequency leakage.

The second stratagem is available only in the feedback topologies. It is to make use of the zeros naturally present in shunt compensation. The procedure has three steps:

1. First, the nominal pole of G_p closest to the band edge is deliberately retained. The remainder of G_p is approximated by a single second order element (as before), on the basis of the remaining G_p' at the zone edge and the remaining slope g_1' at d.c.

2. If the nominal pole pair, call it G_3, is to remain in its natural position at $s^*=\pm j3a$, it is retained with its full residue and assigned the same nominal *b* as a main pole. However, the *b* may be lowered to achieve a deeper zero.

3. The frequency of G_3 can be moved without affecting either the $Re(G_p)$ or the slope of $Im(G_p)$ at the zone edge if the residue and the damping are both adjusted in the ratio Γ

$$\Gamma = ((\omega_3-\omega_0)/4a)^2 \qquad (34)$$

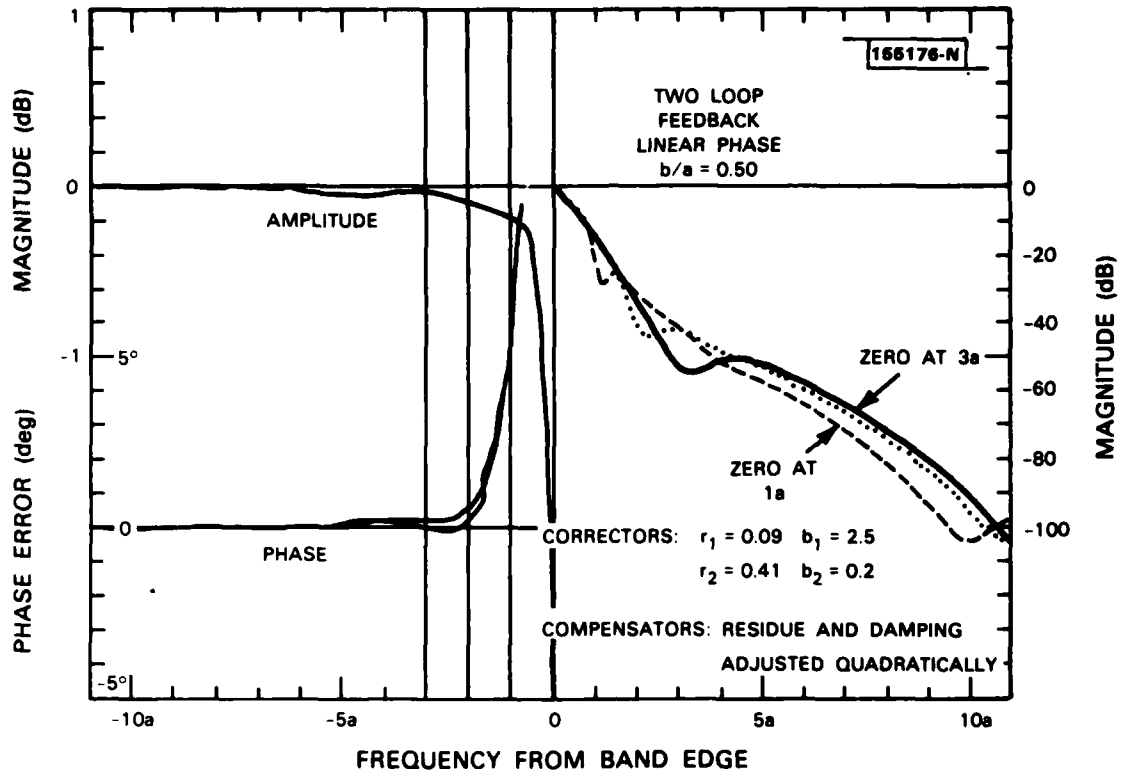

Figure 15. Response of feedback network with selected stop band zeros.

where ω_3 is the frequency location of the zero. Other amplitude adjustment rules are possible; this one has the advantage of not introducing major additional phase distortion near the band edge.

Figure 15 shows the results of applying this algorithm to the location of zeros for main pole b/a=½, with a two pole corrector whose parameters are specified in Table 1 . The Figure shows the transmission for the two loop topology of Figure 5.

Section 8

DOUBLE FEEDBACK CONFIGURATION

The transmission shown for the (single loop) feedback configuration of Figure 13 exhibits an "ear" at the band edge for b/a=0.25 in the single loop topology. Such ears appear to be an unavoidable part of the single loop transmission for b/a less than about one–third.

The cure utilized in the original paper was to drive the network from a finite impedance, rather than zero impedance source. This approach had several advantages:

1. A low loss network could be designed to operate between a resistive source and a resistive load.

2. The transmission "ears" go away.

3. When source and load resistance are taken equal, the pass–band transmission is insensitive to minor variations of individual components.

4. The zeros of transmission are deeper than with the zero impedance source.

Most of these advantages remain when the mathematics is realized in the two loop topology shown in Figure 5. Figure 16, for example, is the transmission of a two loop network with the same parameters as single loop Figure 13. Note that the peaks in transmission at the band edge are gone.
In the two loop topology of Figure 5, the elements G are used three times. As a result

1. There are two more amplifiers and two more sets of elements G_p than in the single loop case.

2. An unbalance in two nominally equal branch G_p's, actually realized along with the Y's, is equivalent to an adjustment in Y_C. This can be an extra degree of freedom in the design of the corrector, or source of error in realization.

The extra depth of zeros in the two loop topology is the result of all signal paths having to pass through an equivalent "G" element twice. This advantage is accompanied by a potential 6 dB *increase* in the transmission at other stop band frequencies. This increase can be deduced by considering the ratio θ_{21} of the two loop transmission (from Eq (4) to the one loop transmission (from Eq (3)), normalized so that $|\theta_{21}|\to 1$ within the pass band

$$\theta_{21} = 2G_0(Y_A+Y_B)/(G+2Y_A)(G+2Y_B) \qquad (35)$$

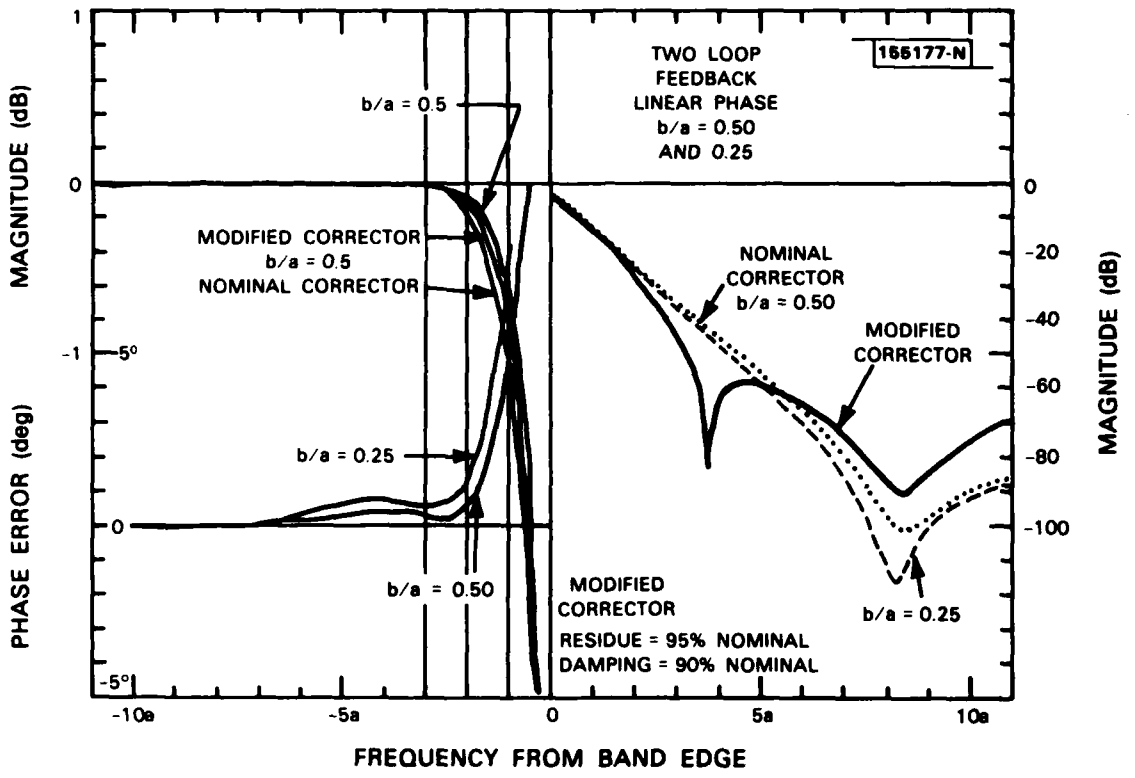

Figure 16. Two loop transmission.

In the stop band, Y_A and Y_B tend to zero, while away from its poles G tends to G_0. Thus, asymptotically, θ_{21} tends to 2, which is 6 dB in power. However, much of this asymptotic region of lower attenuation is far enough away from the band edge so that theoretical 6 dB has little practical significance. The "matched source" configuration remains the topology of choice if lumped passive components can be used. [9] The double feedback loop also appears to be the topology of choice for critical active circuit applications. Otherwise, the single loop is to be preferred over the simple topology for most active circuit realizations.

---

[9] The main pole on the real axis contributes an inductor to the branch admittance, which can be combined with the ideal transformer to produce a real transformer. In the context of the original paper, if the inductances of the other branches y_i are all L, then this "d.c." inductance is 2L.

Section 9

TYPICAL CIRCUITS

Although the theoretical network building block is the individual pole and residue, the physical building block is the sum of a given upper half plane pole and its complex conjugate mate. If the position of the uhp pole is at s=jma+b, then the physical building block is $y_{mo}(s)$ if the number of main poles is odd; and y_{me} if M is even.

$$y_{mo}(s) = b(s+b)/(s^2 + m^2a^2 + b^2 + 2bs) \quad \text{(a)}$$

$$y_{me}(s) = jmab/(s^2 + m^2a^2 + b^2 + 2bs) \quad \text{(b)}$$

(36)

Note that the frequency s=jma is not a good place to align either of these 2nd order systems. For M odd, a good alignment frequency is ω_{mo}:

$$\omega_{mo} = (m^2a^2 - b^2)^{1/2} \quad (37)$$

where the phase and magnitude of the transmission are zero degrees and unity, respectively. For M even, a good alignment frequency is ω_{me}

$$\omega_{me} = (m^2a^2 + b^2)^{1/2} \quad (38)$$

where the phase and transmission are 90° and $m/\sqrt{(m^2+b^2)}$, respectively.

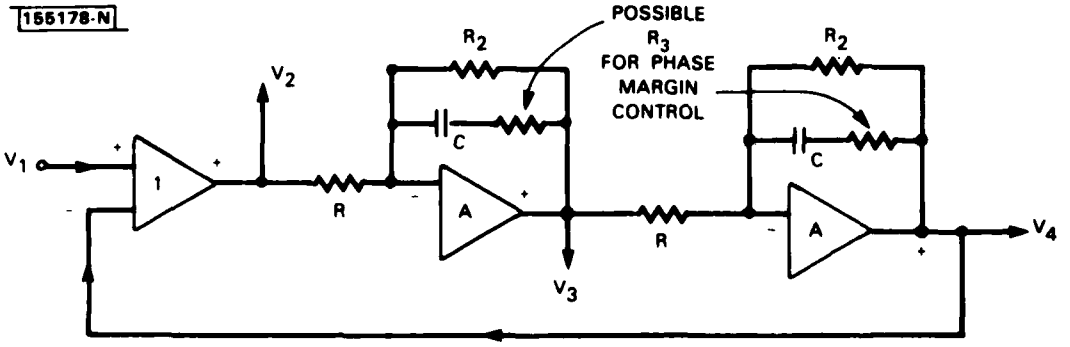

Figure 17. Circuit with R-C controlled resonant frequency.

It is not the objective here to exhibit the "best" circuit for a particular purpose, merely one that is convenient. Here, "convenient" is taken to mean a circuit in which there is (at least in principle) some independence in adjusting the *b* parameter and the ω–position of a given pole.

9.1 R–C CIRCUIT

One such circuit is shown in Figure 17. It uses nominal negative feedback which becomes positive feedback near resonance. The transmission of this second order system from an input V_1 to outputs V_2, V_3, and V_4 are

$$V_2/V_1 = (s+e)\,2/(s^2+2es+g^2) \quad \text{(a)}$$

$$V_3/V_1 = \kappa\,\omega_m\,(s+e)/(s^2+2es+g^2) \quad \text{(b)}$$

$$V_4/V_1 = \kappa^2\,\omega_m{}^2/(s^2+2es+g^2) \quad \text{(c)}$$

(39)

where the various parameters in Eq (39) are given by

$$\kappa = A/(1+A)$$

$$\omega_m = 1/RC$$

$$e = 1/R_2C + \omega_m/(1+A)$$

$$g^2 = e^2 + \omega_m{}^2\,\kappa^2 \quad (40)$$

These equations should be compared with Eqs (36). The obvious choices are to use V_3 as the output with the odd pole configuration, V_4 with an even pole configuration. However, each of these outputs requires attenuators to equalize an extra factor of ω_m in Eqs (40b) and (40c).

With the main poles, the preferable alternative is to use V_2 for the odd pole configuration, V_3 for the even pole configuration. This leaves all of the contributions high by a factor of (s+e). For the main poles, a single overall equalization b/(s+b) is easier to implement than individual equalization of the ω_m. On the other hand, the amplitudes of the corrector and compensation poles need adjustment. Unless they have the same damping as the main poles, they are best obtained from V_3 (or V_4), and equalized for combination with the result of the main pole synthesis. The possibility of such diversity in realization is one of the advantages of the pole–residue approach.

The poles of the transmission given in Eqs (39) are at frequencies s_m

$$s_m = 1/R_2C + \omega_m/(A+1) \pm j\omega_m \quad (41)$$

To the extent that the open loop op–amp gains A can be made much larger than the ratio ma/b at resonance

1. RC determines *ma*.

2. R_2C determines *b*.

3. The adjustments of *e* to *b* and g^2-e^2 to m^2a^2 are independent of one another.

Inasmuch as all the b's are close to being equal, an efficient alignment procedure is to fix R_2 and C, while adjusting R for the individual frequency. (This process remains convenient for a switchcap equivalent to Figure 17.)

The amplification A is in general frequency dependent. Indeed, it is not uncommon for an op–amp to be in the single pole roll–off regime over much of its range of use:

$$1/(1+A) = \delta_0 + s/\omega_u + \text{....higher order terms in } s$$

$$\kappa = \kappa_0 - s/\omega_u + \ldots. \qquad (42)$$

where ω_u is the frequency of projected unit gain. There are two effects.

1. An angle proportional to frequency is introduced into the residues.

2. There is a reduction of the damping.

The former effect merely introduces a slight change in the overall delay of the filter. The latter effect can be large enough to cause oscillation.

A stratagem for avoiding this problem is to use a resistance R_3 in series with C, chosen so that R_3C is $1/\omega_u$. This is not a critical element. It does not much matter whether it is physically in series with C or with the parallel combination of R_2 and C.

9.2 SWITCHCAP ADAPTATION

In integrated circuits it may be inconvenient to obtain and trim resistors to precise stable values. The substitute is the switched capacitor. Figure 18a shows such a capacitor used to replace a resistor otherwise bridged between nodes "A" and "B". In the simplest case, the impedance looking out into both nodes is low enough so that the settling time for charging and discharging the switched capacitor (C_0 in the Figure) is short compared with the time that the switch is closed at either node. The effective conductance of the equivalent resistor bridged between the nodes is *g:*

$$g = C_0 f \qquad (43)$$

where *f* is the switching frequency. When a capacitor C intervenes between one terminal (say, B) and low impedance circuitry (at say, D) then the effective conductance is modified to

$$g = C_0C\ f/(C_0+C) \qquad (44)$$

The prime candidate for switchcap substitutes are the resistors R in Figure 17. The replacement makes the filter pass band programmable by adjustment of the switching

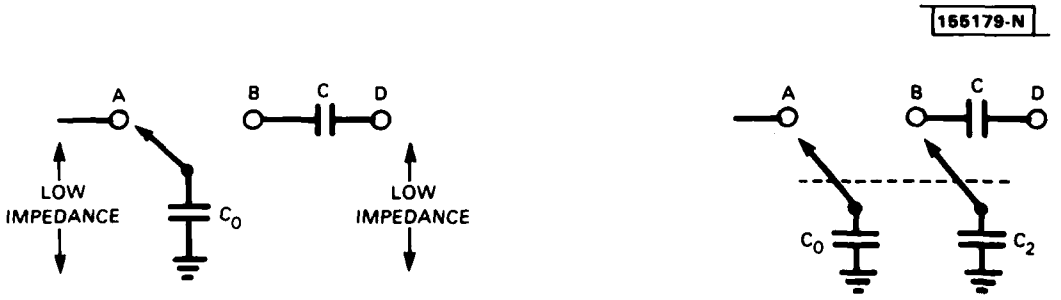

Figure 18. Elimination of resistors by switching capacitors.
(a) Switchcap circuit. (b) Double switching circuit.

rate[8] A second candidate for such replacement is the damping control R_2. Its replacement by a switched capacitor C_2 is shown on the rhs of Figure 18. Since there are now two capacitors switched to node B, it simplifies isolation if they are connected to the node alternately as shown in the Figure.

What are shown as switches in the figure are, in fact, active elements. These must be designed so that the settling time is short compared with the sampling interval. In addition, the closed loop response of the overall system is significant only "at" the sampling times, not between them. As a result, small delays in the closed loop amplifier do not necessarily show up as additional delay in the sampled signal output. Thus, the role of the resistors R_3, which is to compensate for such small delays, may be moot. In any event, the precise value of such resistors is not critical; if needed, they can be realized by any convenient means.

Section 10

SAMPLED DATA FILTERS

Although the *topology* of the z–plane filter has been given, the analysis has been carried out only in the s–plane. That analysis can be extended to the z–plane topology by use of the mapping transformation given in Eq (9). This transformation maps the z–plane filter into *an infinite sequence* of L–Ph filters in the s–plane. One of these is the low pass filter. The remaining filters are "ghosts" whose pass bands and singularities are $2\pi/\tau$ in (radian) frequency apart along the $j\omega$–axis in the s–plane.

There are two aspects to the resulting "aliasing" problem: (a) the cumulative effect of the ghosts within the pass– and stop–bands of the low pass range, and (b) the means by which the transmission at the repeated "ghost" pass bands is supressed. Both effects are met in all sampled data filters, not merely those which happen to be L–Ph. They are treated here in order to better define the circumstances under which the effects of aliasing are in fact negligible for the L–Ph filter.

In a band pass design, the effect of one additional filter at negative frequencies is neglected. For a low pass, the effect of the next adjacent ghost is similarly negligible out to a frequency ω_c corresponding to one–half the sampling rate:

$$\omega_c = \pi/\tau \tag{45}$$

If ω_0=Ma is the band edge of the low pass, then the very terminology "low pass" presumes a stop band wide compared with ω_0, so that

$$\omega_c \gg 2\omega_0 \tag{46}$$

As a result only the *asymptotic* transmission of the ghosts affects the low pass for $\omega<\omega_c$.

For an odd pole number M, the asymptotic transmission has the form $\epsilon b(s-s_n)^{-1}$, where s_n is at the center of the *n*th ghost. This asymptotic form arises because for odd M the sum of residues from all poles is not automatically zero. There will be a finite remainder ϵ, whether by deliberate choice or by random errors in adjustment of drift of individual components. Let $\eta(s)$ be the cumulative additive effect of the ghosts. Within the low pass range, $\eta(j\omega)$ is mainly imaginary.

In the pass band,$\eta(s)$ can be estimated by the same methods used to estimate G(s) above. Near the s–plane origin

$$d\eta/ds = \epsilon b /12\omega_c^2 \tag{47}$$

Since $\omega_c>2\omega_0$, the effect in the pass–band cannot be greater than $\epsilon b/24Ma$, generally less than a fraction of a percent. Thus the ghosts can be neglected in the pass–band. For the stop–band, the effect of the ghosts is largest at $\omega=\omega_c$. At ω_c, the effect can be estimated by a direct sum of the contributions:

$$\eta(j\omega_c) = j\epsilon b \Sigma[1/(^2n\omega_c-\omega_c) - 1/(2n\omega_c+\omega_c)]$$

$$= (j\epsilon b/\omega_c) \Sigma\ 1/(n^2-1) \qquad n \geq 1$$

$$= .5708\ j\epsilon b/2Ma \tag{48}$$

In this case, some care must be exercised to be sure that the combination of ϵ and M is appropriate to maintaining the desired transmission floor in the face of the ghost contribution.

A final concern is the supression of input frequency components which happen to lie in the ghost pass-bands. Ultimately, a true analog filter is required to eliminate such components from a non-sampled data signal. However, it is a filter whose band edge can be anywhere between ω_0 and ω_c. No serious demands are made on the transition region of this analog filter; it need contain only a few pole pairs.

The switchcap technique for realizing 2nd order operations is a digital-analog hybrid in which the samples are *held* between sampling instants. The result is to multiply the periodic s-plane spectrum by a sinx/x whose zeros are exactly at the centers of the ghost pass-bands along the $j\omega$-axis.[10]

At the edges of the ghost bands, the transmission is bounded by that of the closest edge of the nearest ghost to T_{ghost}

$$T_{ghost} = \pi\ \omega_0\ /2\omega_c \tag{49}$$

T_{ghost} can be made arbitrarily small by raising the sampling rate so that ω_c is arbitrarily high. However, the sampling rate may be fixed by practical considerations; in such cases the additional analog filter at the input is inavoidable.

---

[10] With a periodic spectrum this multiplication by sinx/x does not produce divergence as $s \to \pm\infty$; the periodic filter response decreases exponentially in this limit more strongly than the $\sinh\sigma/\sigma$ increases.

Section 11

DISCUSSION OF RESULTS

The question most often asked about the Linear Phase Filter is, "how does it compare with a standard Butterworth or Tchebychef design plus all-pass phase equalization?"

The comparisons made in the text between the simple L-Ph filter and the Tchebychef, and also between the feedback filter and the Butterworth, should suffice for the phase equalization comparison. The comparison is most favorable when the tolerable amplitude and phase errors over most of the pass band are small, so that Tchebychef, Butterworth, and L-Ph design procedures yield nearly the same results for the first 50 dB or so of stop band attenuation. For such cases, the L-Ph filter needs no phase equalization in the pass band, yet has as few, or fewer, second order elements than the unequalized competition.

Another questions is, "what are the disadvantages of these filters?" The answer depends on the application and the components to be used.

One potential disadvantage of the L-Ph designs is that they all achieve part of their stop band attenuation by balance between Y_A and Y_B. These two transmissions must be made of components that drift alike with temperature and time. In particular, they should be mounted on the same chip symmetrically with respect to sources of heat.

Note that the figures in the text are all normalized to unity transmission at d.c. The absolute transmissions of the simple filters are low, a consequence of $b/a \geq 1$ as shown in Figure 8. As a result, these filters are more sensitive to drift than the loop topologies for which b/a can be taken as close to zero as the stability of components permits.

Another potential disadvantage is that most L-Ph designs have floors (or at least landings on a descending ramp) to the stop band transmission. It is important to recognize that such floors also arise from what is practical in the isolation of input from output in a single filter chip or box, regardless of theoretical transmission. Such isolation floors range from as little as 40 dB to as much as 70 dB, depending on the frequency range and the technology available. The fact that individual L-Ph filters have theoretical floors or landings in the same range cannot be counted as a severe additional disadvantage. The cure is in both cases the same: if more isolation is necessary, use two stages in cascade.

It is sometimes asked, "how well do these filters conform to a suitable set of theoretical limitations?"

> Such questions can be answered only in the context of additional intellectual assumptions or esthetic standards. A framework for such discussions was provided in the subsection on multiple pole correctors in the form of a transition zone within which the transmission is only loosely controlled. However, a detailed discussion of the topic is beyond the scope of the present study.

A final question is "why aren't these L-Ph designs more widely used?"

> The answer is essentially beaurocratic. Filter specifications are written with other filters in mind; enough features of such other filters are specified to make the use of any other filter, including the L-Ph filter, awkward.

The problem of specification is two-fold, amplitude and phase. The amplitude specification problem is merely one of making engineers aware of the fact that for a small adjustment of their transmission template, they can get L-Ph "for free".

Most of the examples given in this report easily fit the amplitude template shown in Figure 1. This template differs from the template that might accompany a Butterworth or Tchebychef design in

a) Specifying a 1 dB (5° phase distortion) point instead of a 3 dB point.

b) Allotting more space between the in-band limits and the 1 dB point than is typical of Butterworth or Tchebychef designs.

c) Allowing an isolated deep stop band zero (carrier supression) up to the edge of the transition zone.

d) Not specifying stop band attenuation deeper than fixed floor from a single stage filter.

From several of the specific designs that appear in the text, it is evident that the template is conservative. The floor on the progression of band-edge carrier-supression zeros is based on nominal damping for a nominal out-of-band zero. If further in-band phase distortion is tolerable, or if higher Q's are practical for the zero, then this floor is lowered.

The phase template for these filters is the same as the amplitude template, except that the 1 dB point is replaced by the 5° or 0.1 radian point. There is also no specification of the phase beyond this point. The specification of phase is made difficult by the common use of "group delay" defined as the frequency derivative of phase. Regrettably, "group delay" so defined has no physical significance when the phase distortion is low. [11] Yet group delay (by derivative) distortion is almost always specified.

---

[11] Group delay acquires physical meaning when the Fourier transform for the impulse response can be found by the method of stationary phase integration. This requires that the phase distortion be *high*, amounting to at least *several radians* across the frequency bandwidth of the "group" being considered.

These filters behave in the pass–band like a piece of cable with a fixed delay and small impedance mismatches at the two ends. In the simple topology, the effective mismatch is inherent, producing the periodic errors discussed in Section 4. In the loop topologies, the transmission line is theoretically terminated at one (single loop) or both (two loop) end(s). In the loop topologies, mis–settings of gains G_0 will cause the mismatches to return. As a result of the mismatches, there are internal reflections which are small, broadband, and circulate with decreasing amplitude at each bounce. The delay of the primary echo is simply triple travel; higher order echos have correspondingly longer multiple travel delays.

How big an echo can one tolerate? That depends on the application. In an audio channel a broad band 30 ms echo down 6 dB is scarcely distinguishable from the environment by the ear, but is disastrous to digital data transmission. On the other hand a 1 s echo down 30 dB can be disastrous to listening (or speaking) and scarcely noticable in its effect on digital data transmission. To multiply the 1 s echo by its amplitude and announce a 30 ms delay distortion is not only absurd: it leads to the wrong engineering conclusions. Yet this is exactly what a "group delay distortion" calculation does.

A solution to the phase distortion specification problem is to specify the phase distortion in two parts

a) Recognizable broad band echos, and

b) Other sources of delay distortion.

Examination of the Figures in this report reveals that the pass band amplitude and phase ripple are strongly correlated. This is because both consist almost entirely of broadband echos. Thus, the phase distortion can be specified by echo amplitude or by radian error; but the amplitude of the identifiable echo can be frequency dependent. The "other sources" of delay distortion are not significant to within *a* units of the in–band zone edge.

It is now more than thirty years since the writer built his first L–Ph band–pass and low–pass filters. The statements made in his 1964 paper are still valid: if there is a use for these designs, they will be used; if not, they won't be. The only valid concern is that these filters be a *known* alternative, so that the design engineer in fact has a choice.

REFERENCES

[1] R.M. Lerner, "Band Pass Filters With Linear Phase," *Proc. IEEE, 52,* pp. 249–268, (March 1964)

[2] R.M. Lerner, "Impulse Noise Suppression Communication System Utilizing Matched Filters and Noise Clipping," U.S. Patent #3,252,093, May 17, 1966

[3] R.M. Lerner, "The Design of a Constant–Angle or Power–Law Magnitude Impedance," *IEEE Trans Circuit Th, CT–10*, pp. 98–107 (March 1963)

[4] B. Gold and J. Tierney, "A Digitized Voice–Excited Vocoder for Telephone Quality Inputs Using Band Pass Sampling of the Baseband Signal," *J. Acous. Soc. Am., 37,* pp.753–754, April 1965, DDC 619923

[5] *Digital Processing of Signals*, Gold and Rader (McGraw–Hill, New York, 1979) §3.5, pp.52–54.

[6] A. DeLagrange, "Bringing Lerner Filters Up to Date; Replace Passive Components With Op–amps," *Electronic Design*, Feb. 15, 1979

[7] K. DeWitt, U.S. Patent #3,727,147, Apr 10,1973

[8] C.A. Lish, "A z Plane Lerner Switched–Capacitor Filter," *IEEE J. Solid State Circ, SC–19*, pp 888–892 (December 1984)

[9] H.W. Bode, U.S. Patent #1,828,454, October, 1931.

[10] L.B.W. Jolley, *Summation of Series, 2nd Ed.* (Dover, New York, 1961) Formulas §769 and §770

[11] Hendrik Bode, *Network Analysis and Feedback Amplifier Design* (Van Nostrand, New York, 1945), Chapts. 13 and 14. Note particularly the historical footnote at the beginning of Chapt. 14.

UNCLASSIFIED

SECURITY CLASSIFICATION OF THIS PAGE *(When Data Entered)*

REPORT DOCUMENTATION PAGE		READ INSTRUCTIONS BEFORE COMPLETING FORM
1. REPORT NUMBER ESD-TR-85-240	2. GOVT ACCESSION NO. AD-A163 984	3. RECIPIENT'S CATALOG NUMBER
4. TITLE *(and Subtitle)* Low Pass Filters with Linear Phase		5. TYPE OF REPORT & PERIOD COVERED Technical Report 6. PERFORMING ORG. REPORT NUMBER Technical Report 729
7. AUTHOR*(s)* Robert M. Lerner		8. CONTRACT OR GRANT NUMBER*(s)* F19628-85-C-0002
9. PERFORMING ORGANIZATION NAME AND ADDRESS Lincoln Laboratory, M.I.T. P.O. Box 73 Lexington, MA 02173-0073		10. PROGRAM ELEMENT, PROJECT, TASK AREA & WORK UNIT NUMBERS Program Element Nos. 63250F
11. CONTROLLING OFFICE NAME AND ADDRESS Air Force Systems Command, USAF Andrews AFB Washington, DC 20331		12. REPORT DATE 12 December 1985 13. NUMBER OF PAGES 48
14. MONITORING AGENCY NAME & ADDRESS *(if different from Controlling Office)* Electronic Systems Division Hanscom AFB, MA 01731		15. SECURITY CLASS. *(of this Report)* UNCLASSIFIED 15a. DECLASSIFICATION DOWNGRADING SCHEDULE

16. DISTRIBUTION STATEMENT *(of this Report)*

Approved for public release; distribution unlimited.

17. DISTRIBUTION STATEMENT *(of the abstract entered in Block 20, if different from Report)*

18. SUPPLEMENTARY NOTES

19. KEY WORDS *(Continue on reverse side if necessary and identify by block number)*

Lerner filter	phase distortion	sampled data filter
linear phase filter	delay distortion	tchebychef filter
low pass filter	non minimum phase	butterworth filter
transmission zeros	switchcap filter	

20. ABSTRACT *(Continue on reverse side if necessary and identify by block number)*

This report is intended as a modern sequel to "Band Pass Filters with Linear Phase", published over 20 years ago. Here, the linear phase algorithms are adapted to low-pass integrated active circuit topologies for potential use as the input filter in sampled data control systems and other low-pass applications for which traditional coil-capacitor-transformer filter designs are no longer appropriate.

The linear phase algorithm is applicable to a variety of circuit topologies which are not mathematically equivalent. Application to the overall transfer funciton (the "simple" approach) results in transmission that is nearly equal-ripple in both amplitude and phase, the errors being equivalent to echos in a misterminated transmission line. The resulting filters compare favorably with modes order Tchebychef filters (lacking phase control). Application to branches of a feedback topology (mathematically equivalent to a lattice) leads to control of echoes and stop-band zeros at the cost of extra elements. In this case, the results compare favorably with ordinary Butterworth filters (lacking phase control) having the same total number of poles.

Practical means for inserting stop band zeros without redesign of the pass-band are considered. Circuits of both the R-C and switchcap types are discussed.

DD FORM 1 Jan 73 1473 EDITION OF 1 NOV 65 IS OBSOLETE

UNCLASSIFIED

SECURITY CLASSIFICATION OF THIS PAGE *(When Data Entered)*

END

FILMED

3-86

DTIC